2016 International Symposium on Nonlinear Theory and Its Applications,
NOLTA2016, Yugawara, Japan, November 27th-30th, 2016

Multi-compartment Neuron Model based on Asynchronous Bifurcation Processor

Taiki Naka† and Hiroyuki Torikai‡

†Department of Computer Science, Kyoto Sangyo University
Motoyama, Kamigamo, Kita-Ku, Kyoto 603-8555, Japan
g1344900@cse.kyoto-su.ac.jp, torikai@cse.kyoto-su.ac.jp

Abstract—In this paper, a multi-compartment neuron model based on the concept of an asynchronous bifurcation processor is studied. It is shown that the model can reproduce typical propagation phenomena of membrane potentials between somas and dendrites of neurons such as forward propagations of action potentials from dendrites and resulting backward propagations of action potentials from a soma. It is also shown that the model can reproduce formations of typical potential gradients in dendrites of neurons.

1. Introduction

A neuron typically consists of dendrites (input cables), a soma (cell body), and axons (output cables), where the dendrite sometimes has complicated physical structure such as the Purkinje cell. A wide variety of dendritic phenomena have been observed [1]-[4], where it has been suggested that such dendritic phenomena play certain roles in neural information processing as well as spike-timing dependent plasticity learning. One of the major modeling methods of the "soma plus dendrite" is a *multi-compartment soma-dendrite modeling method*, i.e., to discretize the dendrite into a set of small compartments and to model the "soma plus dendrite" by a coupled system of the compartments as shown in Fig. 2(b) [5], where each compartment is designed to reproduce nonlinear dynamics of a membrane potential of the corresponding part of the neuron. On the other hand, our group has been developing a neural system modeling approach based on the nonlinear dynamics of an asynchronous cellular automaton, where nonlinear dynamics (especially, bifurcations) of neural systems are reproduced by the asynchronous cellular automaton with low hardware cost [6]-[9]. Our group is conceptually referring to such a hardware platform as "asynchronous bifurcation processor (ABP)." In this paper, a multi-compartment neuron model based on the concept of the ABP [9] is studied. It is shown in this paper for the first time that the model can reproduce typical propagation phenomena of membrane potentials between somas and dendrites of neurons such as forward propagations of action potentials from dendrites and resulting backward propagations of action potentials from a soma. It is also shown that the model can reproduce formations of typical potential gradients in dendrites of neurons.

2. Multi-compartment neuron model based on ABP

Fig. 1(a) shows a basic structure of a multi-compartment neuron model based on the ABP [9]. The model consists of $Q > 0$ compartments $\{C_0, C_1, \cdots, C_{Q-1}\}$, where all the compartments are assumed to be connected (i.e., there is no isolated compartment). The 0-th compartment C_0 is used as a soma compartment and the other compartments $\{C_1, \cdots, C_{Q-1}\}$, are used as dendrite compartments. A dendrite compartment C_i is said to be a terminal compartment if it is connected to exactly one dendrite compartment, e.g., the compartments $\{C_4, C_5, C_7, C_8\}$ in Fig. 1(a) are terminal compartments. As shown in Fig. 1(b), each i-th compartment C_i can accept the following stimulation input (not necessarily).

$$I_i(t) = \begin{cases} 1 & \text{if } t \in \{t_{Ii}^{(1)}, t_{Ii}^{(2)}, \cdots\}, \\ 0 & \text{otherwise,} \end{cases}$$

where $t_{Ii}^{(n)}$ is the n-th spike timing (or rising edges) of the stimulation input $I_i(t)$. As shown in Fig. 1(b), Each i-th compartment C_i has a membrane register storing the following discrete membrane potential.

$$V_i \in \{0, 1, \cdots, N-1\},$$

where the integer parameter $N > 0$ determines the resolution of the discrete membrane potential V_i. Also, each i-th compartment C_i has a recovery register storing the following discrete recovery variable.

$$U_i \in \{0, 1, \cdots, M-1\},$$

where the integer parameter $M > 0$ determines the resolution of the discrete membrane potential U_i. (v)The i-th and the j-th compartments C_i and C_j are connected via discrete conductances $G_{ij} \in \{0, 1, \cdots, L-1\}$ and $G_{ji} \in \{0, 1, \cdots, L-1\}$, where the integer parameter $L > 0$ determines the resolution of the discrete conductances G_{ij} and G_{ji}.Each i-th compartment C_i has the following internal clocks.

$$C_{Vi}(t) = \begin{cases} 1 & \text{if } t \in \{t_{Vi}^{(1)}, t_{Vi}^{(2)}, \cdots\}, \\ 0 & \text{otherwise,} \end{cases}$$

$$C_{Ui}(t) = \begin{cases} 1 & \text{if } t \in \{t_{Ui}^{(1)}, t_{Ui}^{(2)}, \cdots\}, \\ 0 & \text{otherwise,} \end{cases}$$

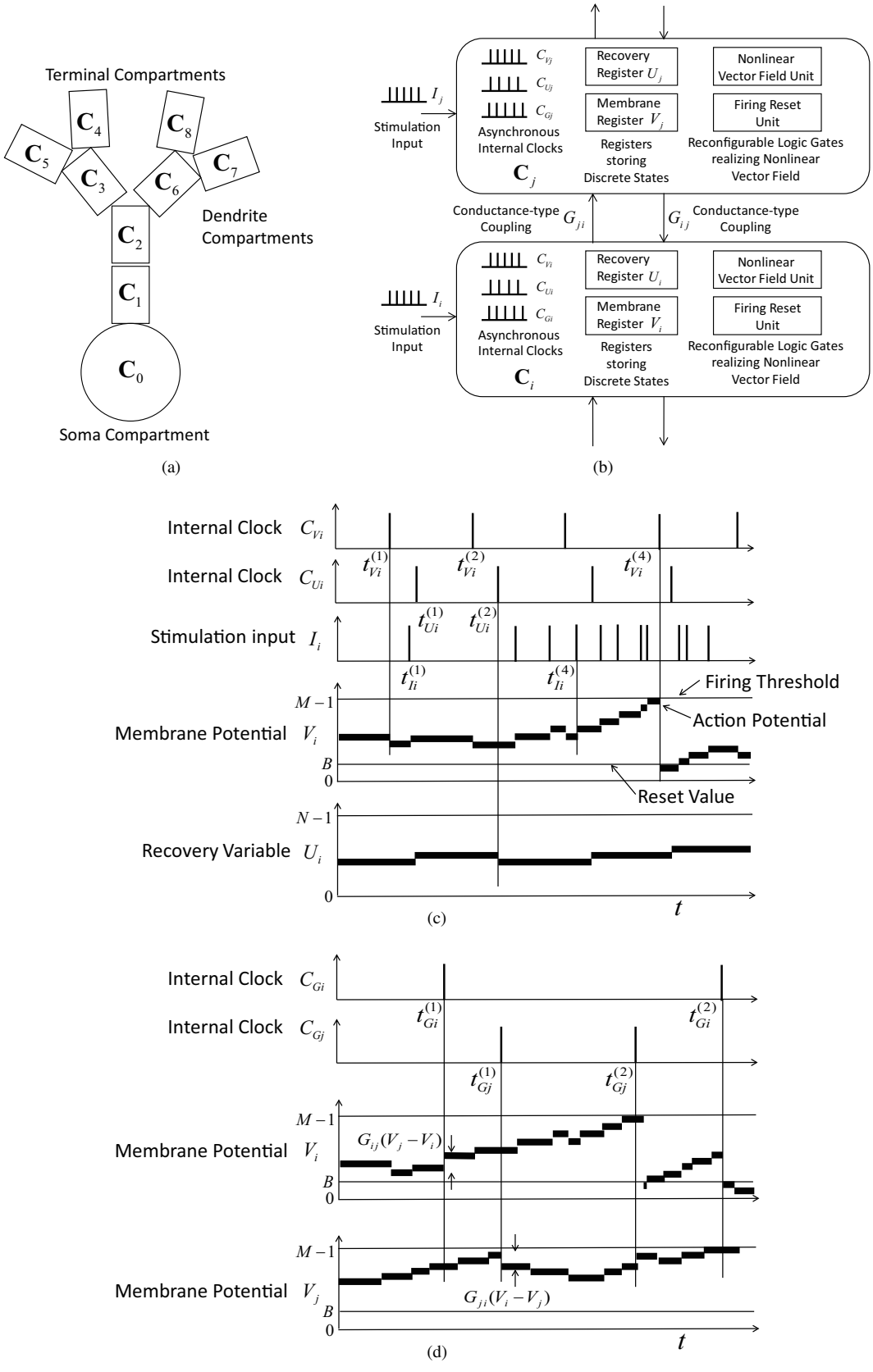

Figure 1: (a) Structure of the multi-compartment neuron model based on the ABP. (b) Connection between the i-th compartment C_i and the j-th compartment C_j via the discrete conductances G_{ij} and G_{ji}. (c) Typical time-waveforms of the i-th compartment. (d) Connection between the i-th compartment C_i and the j-th compartment C_j via the discrete conductances G_{ij} and G_{ji}.

$$C_{Gi}(t) = \begin{cases} 1 & \text{if } t \in \{t_{Gi}^{(1)}, t_{Gi}^{(2)}, \cdots\}, \\ 0 & \text{otherwise,} \end{cases}$$

where $t_{Vi}^{(n)}$, $t_{Ui}^{(n)}$, and $t_{Gi}^{(n)}$ represent spike timings (or rising edges) of the clocks. Let t^+ denote $\lim_{\epsilon \to +0} t + \epsilon$ (i.e., just after t). The internal clocks C_{Vi} and C_{Ui} trigger the following asynchronous transitions of the discrete states V_i and U_i, respectively (see for example V_i at $t = t_{Vi}^{(1)}$ and U_i at $t = t_{Ui}^{(2)}$ in Fig. 1(c)).

$$\begin{aligned} V_i(t^+) &= V_i(t) + D_V(V_i, U_i) \ \text{ if } \ C_{Vi}(t) = 1, \\ U_i(t^+) &= U_i(t) + D_U(V_i, U_i) \ \text{ if } \ C_{Ui}(t) = 1, \end{aligned} \tag{1}$$

where $D_V(V_i, U_i)$ and $D_U(V_i, U_i)$ are discrete functions defined by

$$\begin{aligned} &D_V(V_i, U_i) = 1 && \text{if } (V_i, U_i) \in \mathbf{S}_i^{++} \cup \mathbf{S}_i^{+-}, \\ &D_V(V_i, U_i) = -1 && \text{if } (V_i, U_i) \in \mathbf{S}_i^{-+} \cup \mathbf{S}_i^{--}, \\ &D_V(V_i, U_i) = 0 && \text{if } (V_i, U_i) \in \mathbf{S}_i^{0}, \\ &D_U(V_i, U_i) = 1 && \text{if } (V_i, U_i) \in \mathbf{S}_i^{++} \cup \mathbf{S}_i^{-+}, \\ &D_U(V_i, U_i) = -1 && \text{if } (V_i, U_i) \in \mathbf{S}_i^{+-} \cup \mathbf{S}_i^{--}, \\ &D_U(V_i, U_i) = 0 && \text{if } (V_i, U_i) \in \mathbf{S}_i^{0}, \end{aligned}$$

$$\begin{aligned} &\mathbf{S}_i^{++} \equiv \{(V_i, U_i) | U_i < f_V(V_i), U_i \le f_U(V_i)\}, \\ &\mathbf{S}_i^{-+} \equiv \{(V_i, U_i) | U_i \ge f_V(V_i), U_i < f_U(V_i)\}, \\ &\mathbf{S}_i^{+-} \equiv \{(V_i, U_i) | U_i \le f_V(V_i), U_i > f_U(V_i)\}, \\ &\mathbf{S}_i^{--} \equiv \{(V_i, U_i) | U_i > f_V(V_i), U_i \ge f_U(V_i)\}, \\ &\mathbf{S}_i^{0} \equiv \{(V_i, U_i) | (V_i, U_i) \notin \mathbf{S}_i^{++} \cup \mathbf{S}_i^{+-} \cup \mathbf{S}_i^{-+} \cup \mathbf{S}_i^{--}\}, \end{aligned}$$

where f_V and f_U are discrete functions defined by

$$\begin{aligned} &f_V(V_i) = \alpha(\lfloor k_1 (V_i)^2 + k_2 V_i + k_3 \rfloor), \\ &f_U(V_i) = \alpha(\lfloor k_4 V_i + k_5 \rfloor), \\ &k_1 = \tfrac{f_1 M}{N^2}, \ k_2 = -2k_1 \lfloor f_2 N \rfloor, \\ &k_3 = k_1 (\lfloor f_2 N \rfloor)^2 + \lfloor f_3 M \rfloor, \ k_4 = \tfrac{f_4 M}{N}, \ k_5 = \lfloor f_5 M \rfloor, \end{aligned}$$

where $\lfloor \cdot \rfloor$ is the floor function, $\alpha(x) = x$ for $-1 \le x \le M$, and $\alpha(x) = -1$ for $x < -1$. The stimulation input I_i triggers the following asynchronous transition of the membrane potential V_i (see for example V_i at $t = t_{Ii}^{(4)}$ in Fig. 1(c)).

$$V_i(t^+) = V_i(t) + 1 \ \text{ if } \ I_i(t) = 1. \tag{2}$$

In addition, the compartment exhibits the following firing reset (see for example V_i at $t = t_{Vi}^{(4)}$ in Fig. 1(c)).

$$V_i(t^+) = B \ \text{ if } \ V_i(t) = M - 1 \ \text{ and } \ C_{Vi}(t) = 1, \tag{3}$$

where $B \in \{0, 1, \cdots, N-1\}$ is the value to which the membrane potential V_i is reset. When the compartment exhibits the above firing reset, the compartment is said to generate an action potential of V_i as show in Fig. 1(c). In this paper we fix the parameter values to $(N, M, f_1, f_2, f_3, f_4, f_5, B) = (64, 64, 3.5, 0.45, -0.05, 1.5, -0.43, 10)$. Now, let us consider the connection of the compartments shown in Fig. 1(b). The internal clock C_{Gi} triggers the following asynchronous transition of the membrane potential V_i (see Fig. 1(d)).

$$V_i(t^+) = V_i(t) + G_{ij}(V_i, V_j)(V_j(t) - V_i(t)) \quad \text{if } \ C_{Gi} = 1, \tag{4}$$

where

$$G_{ij}(V_i, V_j) = \begin{cases} 1/8 & \text{if } -30 \le |V_i - V_j| \le 30, \\ 0 & \text{otherwise.} \end{cases}$$

For example, at $t = t_{Gi}^{(1)}$ in Fig. 1(d), the membrane potential V_i increases by $G_{ij}(V_j - V_i)$ since $V_j > V_i$. Also, at $t = t_{Gj}^{(1)}$, the membrane potential V_j decreases by $G_{ji}(V_i - V_j)$ since $V_i < V_j$. Fig. 3 shows reproductions of typical dendritic phenomena by the multi-compartment neuron model based on the ABP. In Fig. 3(a), weak stimulation inputs I_4 and I_5 are applied to the terminal compartments C_4 and C_5, respectively. In this case, no action potential is evoked but the membrane potentials V_i of the compartments form a potential gradient. In Fig. 3(b), strong stimulation inputs I_4 and I_5 are applied to the terminal compartments C_4 and C_5, respectively. In addition, a weak background noise spike-train n_i is applied to each compartment. In this case, the stimulation inputs I_4 and I_5 evoke action potentials of V_4 and V_5 in the terminal compartments C_4 and C_5, respectively. These action potentials evoke an action potential of V_3 in the dendrite compartment C_3. Repeating such dynamics, the action potential propagates to the soma compartment C_0. In Fig. 3(c), a weak stimulation input I_0 is applied to the soma compartment C_0. In this case, no action potential is evoked but the membrane potentials V_i of the compartments form a potential gradient. In Fig. 3(d), a strong stimulation input I_0 is applied to the soma compartment C_0. In addition, a weak background noise spike-train n_i is applied to each compartment. In this case, the stimulation input I_0 evokes an action potential of V_0 in the soma compartment C_0. This action potential evokes an action potential of V_1 in the dendrite compartment C_1. Repeating such dynamics, the action potential propagates to the terminal compartments C_4 and C_5. In Fig. 3(d), a strong stimulation input I_4 is applied to the terminal compartment C_4 and a weak background noise spike-train n_i is applied to each compartment. In this case, a forward propagation induces generation of an action of the soma compartment C_0 and it induces a backward propagation. Note that such a backward propagation induced by a forward propagation plays important role in an STDP learning.

3. Conclusions

In this paper, the multi-compartment neuron model based on the ABP was studied. It was shown that the model can reproduce typical dendritic phenomena such as the forward propagation of action potentials, the backward propagation of action potentials, and the backward propagation induced by the forward propagation. It is was shown that the model can reproduce formations of the potential gradients. Future problems include development of an ABP-based multi-compartment neuron model with STDP learning capability and development if a large scale network of the ABP-based multi-compartment neuron models. This

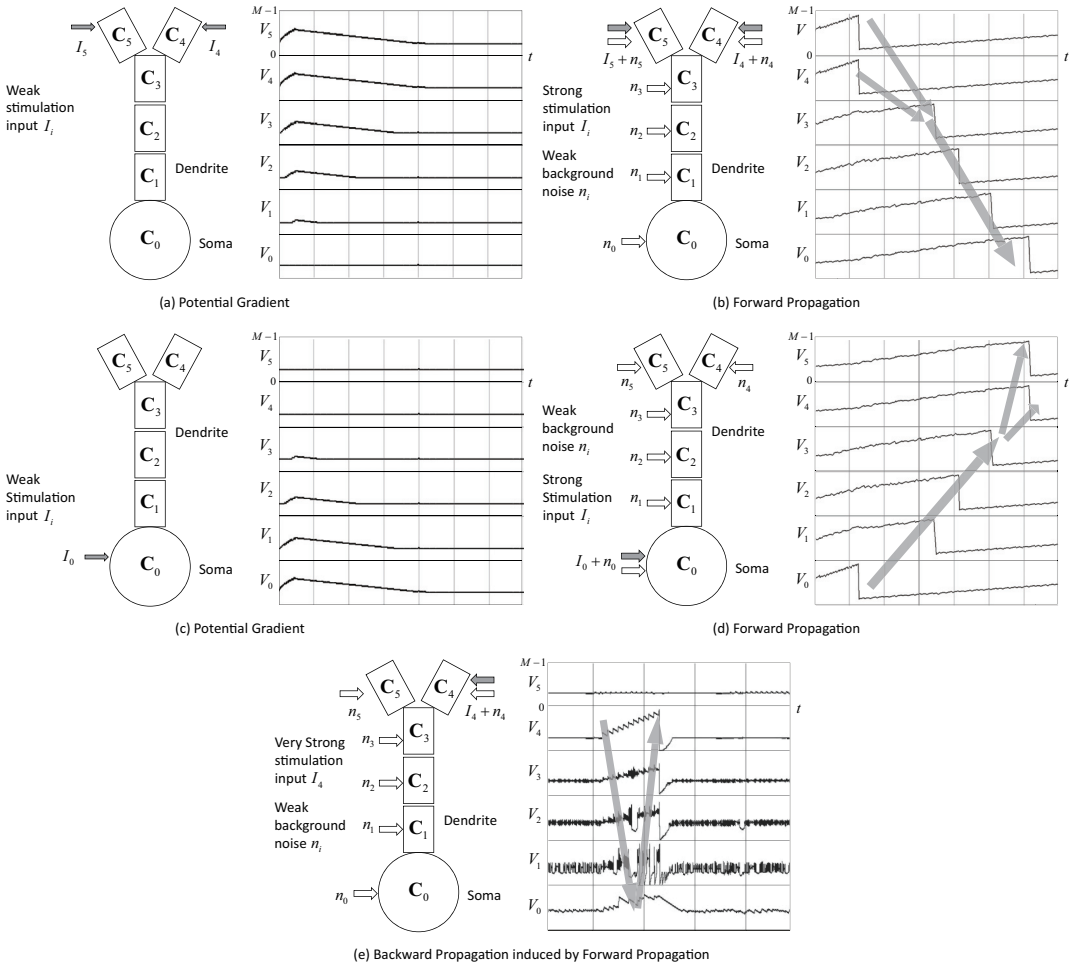

Figure 2: Reproductions of typical dendritic phenomena by the multi-compartment neuron model based on the ABP (simulations). (a) Potential gradient. (b) Forward propagation. (c) Potential gradient. (d) Backward propagation. (e) Backward propagation induced by forward propagation.

work was partially supported by JSPS KAKENHI Grant Number 15K00352.

References

[1] W. Rall, Electrophysiology of a Dendritic Neuron Model, Biophysical Journal, vol. 2, no. 2, pp. 145–167, 1962.

[2] E. Hay, S. Hill, F. Schurmann, H. Markram and I. Segev, Models of neocortical layer 5b pyramidal cells capturing a wide range of dendritic and perisomatic active properties, PLoS Computational Biology, vol. 7, no. 7, e1002107, 2011.

[3] P. J. Sjostrom, E. A. Rancz, A. Roth, and M. Hausser, Dendritic Excitability and Synaptic Plasticity, Physiological Reviews, vol. 88, no. 2, pp. 769–840, 2008.

[4] W. R. Chen, J. Midtgaard, and G. M. Shepherd, Forward and Backward Propagation of Dendritic Impulses and Their Synaptic Control in Mitral cells, Science, vol. 278, no. 5337, pp. 463–467, 1997.

[5] E. M. Izhikevich, Dynamical Systems in Neuroscience, The MIT Press, 2010.

[6] N. Shimada and H. Torikai, A Novel Asynchronous Cellular Automaton Multi-Compartment Neuron Model, IEEE Trans. CAS-II, VOL. 62, NO. 8, pp. 776-780 (2015)

[7] K. Isobe and H. Torikai, A novel hardware-efficient asynchronous cellular automaton model of spike-timing dependent synaptic plasticity, IEEE Trans. CAS-II (accepted)

[8] T. Matsubara and H. Torikai, An Asynchronous Recurrent Network of Cellular Automaton-based Neurons and its Reproduction of Spiking Neural Network Activities, IEEE Trans. NNLS (accepted)

[9] N. Jodai and H. Torikai, A Hardware-Efficient Multi-Compartment Soma-Dendrite Model based on Asynchronous Cellular Automaton Dynamics, Proc. IJCNN, pp. 219-226, 2016.